HIV-specific cytotoxic T-cells in HIV-exposed but uninfected Gambian women

S. ROWLAND-JONES, J. SUTTON, K. ARIYOSHI, T. DONG, F. GOTCH, S. MCADAM, D. WHITBY, S. SABALLY, A. GALLIMORE, T. CORRAH, M. TAKIGUCHI, T. SCHULTZ, ANDREW MCMICHAEL & H. WHITTLE

Nature Medicine **1**, 59–64, 1995.

An error in typography resulted in the incorrect printing of m for the Greek character μ. *Nature Medicine* regrets the errors, which misrepresented the **peptide concentrations** used; the corrected text is below. Please note the name Andrew McMichael, which was misspelled.

Fig. 1 caption: CTL assays were performed . . .pulsed with each of the peptides and a control peptide at a concentration of 10 μm.
Fig. 2 caption: CTL assays were performed . . .pulsed for one hour with each of the peptides and a control influenza peptide at 10 μm.
Methods, paragraph 2: Standard chromium-51 release assays were performed after two weeks using HLA-B35-matched or control mismatched target B-lymphoblastoid cell lines (B-LCLs) labelled with chromium-51 and pulsed with each of the HIV peptides or a control influenza peptide at a concentration of 10 μM.
Methods, paragraph 3: Their cells were pulsed as a pellet for 1 hour with 100 μM of each B35-restricted peptides from HIV-1 and -2, or the previously identified B53-restricted peptide from HIV-2 (ref. 29), at a concentration of 100 μM, then diluted in R/10 to a final concentration of 10 μM and cultured at 2 x 10^6 cells per well in a 24-well Costar plate.
Methods, paragraph 5: Peptide-stimulated cultures using HIV peptides were set up from known seropositive donors with **HLA-B35 or B53** and a control group of volunteers at low-risk of HIV infection. [A typographical correction is in bold type.]

Antifibrinolytic activity of apolipoprotein(*a*) *in vivo*: Human apolipoprotein(*a*) transgenic mice are resistant to tissue plasminogen activator-mediated thrombolysis

T.M. PALABRICA, A.C. LIU, M.J. ARONOVITZ, B. FURIE, R.M. LAWN & B.C. FURIE

Nature Medicine **1**, 256–259, 1995.

Part of the **Methods** section was not printed and appears below. *Nature Medicine* regrets the omission.

Preparation of ^{99m}Tc-labelled human plasma clots. Platelet-rich plasma clots containing a radiotracer were prepared by incorporating ^{99m}Tc-labelled antifibrin-specific antibodies into the clot. $F(ab')_2$ fragments of T2G1s, a monoclonal antifibrin antibody that does not bind to fibrinogen or murine fibrin[24], were labelled with ^{99m}Tc as previously described[25]. The ^{99m}Tc-labelled $F(ab')_2$ fragment of T2G1s (500 μCi) was added to 0.5 ml of human platelet-rich plasma followed by addition of bovine thrombin (100 μl, 3 NIH units ml^{-1}, 0.5 M $CaCl_2$, 0.9% NaCl; Sigma). The plasma reaction mixture was immediately aspirated into two 10-cm lengths of silastic tubing (0.024/0.012", OD/ID) and allowed to clot for 10 min at 37 °C. The radioactivity within the catheter was quantitated and the tubing cut so that each catheter contained approximately 8,000 c.p.m. of ^{99m}Tc.
Murine pulmonary embolus model. Experiments were performed in apolipoprotein(*a*) transgenic mice and their normal littermates. The apolipoprotein(*a*) transgenic mice were created in a hybrid mouse strain produced by crossing strains SJL and C57Bl/6. The transgenic mice express apolipoprotein(*a*) in all tissues examined including liver, plasma, kidney, heart, brain, testis and white fat[7]. Plasma apolipoprotein(*a*) concentration in the transgenic mice used in these experiments averaged 8 ± 1.6 mg dl^{-1}. Apolipoprotein(*a*) circulates largely uncomplexed with lipoproteins. The apolipoprotein(*a*) transgenic mice fed an atherogenic diet are more susceptible than normal mice on the same diet to atherogenesis and the apolipoprotein(*a*) is associated with lipid deposits in the artery wall[6]. Preliminary studies in our model indicated that diet did not influence the effect of apolipoprotein(*a*) on thrombolysis, and all animals were maintained on normal mouse diet.

Pulmonary emboli were generated in pairs of male apolipoprotein(*a*) transgenic[6,7], and littermate control male mice by injection of clotted human platelet-rich plasma in an adaptation of the method of Collen and co-workers[9,10]. After anaesthesia with an intraperitoneal injection of Nembutal (60 mg kg^{-1}) and Ketamine (10 mg kg^{-1}), a longitudinal incision was made over the right jugular vein. The right jugular vein was cannulated with the silastic catheter containing the ^{99m}Tc-labelled plasma clot using ×8 loop magnification. The catheter was advanced 1 to 2 cm into the right atrium of the heart and secured with nylon ligatures. The clot was injected with 0.2 ml of 0.9% NaCl. Subsequent to injection of the clot each animal received a bolus injection of heparin (1,000 IU kg^{-1}) through the right jugular vein catheter. Recombinant tPA was diluted to a total volume of 90 μl in 0.15 M NaCl/0.01% Tween 80/0.2 M arginine. The dose as indicated was infused over 60 min via the right jugular vein catheter using a Harvard constant-rate infusion pump. Images of the ^{99m}Tc-labelled embolized clots were obtained with an Ohio Nuclear series 100 gamma camera equipped with a medium-energy, high-resolution, parallel-hole collimator with a 20% window and were interfaced with a Macintosh computer equipped with Gamma 11 software (Strichman Medical) employing a 124 × 124 matrix mode. Four 5-min baseline scans were obtained before the injection of heparin and the infusion of tPA. Twelve serial 5-min images were obtained during the course of tPA infusion. Upon completion of the experiment, animals were killed by an intravenous overdose of Nembutal.

Rotenoids mediate potent cancer chemopreventive activity through transcriptional regulation of ornithine decarboxylase

C. GERHÄUSER, W. MAR, S.K. LEE, N. SUH, Y. LUO, J. KOSMEDER, L. LUYENGI, H.H.S. FONG, A.D. KINGHORN, R.M. MORIARTY, R.G. MEHTA, A. CONSTANTINOU, R.C. MOON & J.M. PEZZUTO

Nature Medicine **1**, 260–266, 1995.

In **Table 1**, in which the biological activities of *Mundulea sericea* bark ethyl acetate extract and the structure of four rotenoids (1–4) are described, the correct description of the variable groups at the R_1 and R_2 positions was erroneous in two cases. The correct descriptions, in bold type, are as follows: deguelin (1) R_1 = **H**, R_2 = H; tephrosin (2) R_1 = OH, R_2 = **H**; (–)-13α-hydroxytephrosin (3), R_1 = OH, R_2 = OH; (–)-13α-hydroxydeguelin (4), R_1 = H, R_2 = OH. Also, the preparation of the ethyl acetate extract of *M. sericea* bark was previously described in ref. 13 as stated in the Methods section, not reference 14 as stated in the notes to the Tables.

The paternal inheritance of the centrosome, the cell's microtubule-organizing center, in humans, and the implications for infertility

CALVIN SIMERLY, GWO-JANG WU, SARA ZORAN, TERI ORD, RICHARD RAWLINS, JEFFREY JONES, CHRISTOPHER NAVARA, MARYBETH GERRITY, JOHN RINEHART, ZVI BINOR, RICARDO ASCH & GERALD SCHATTEN

Nature Medicine **1**, 47–52, 1995.

Figure 3 was unclear and is reprinted here with the caption. *Nature Medicine* regrets the poor quality of the original figure.

Glycosylation changes of IgG associated with rheumatoid arthritis can activate complement via the mannose-binding protein

R. MALHOTRA, M.R. WORMALD, P.M. RUDD, P.B. FISCHER, R.A. DWEK & R.B. SIM

Nature Medicine **1**, 237–243, 1995.

In this article, Fig. 2 was inadvertently published upside down and without the labels *a* and *b*. *Nature Medicine* regrets this error. The author corrects the figure caption to read: in *b*, Asn 297 is shown as yellow balls and sticks, the α(1–6) arm terminal galactose as orange balls and sticks.

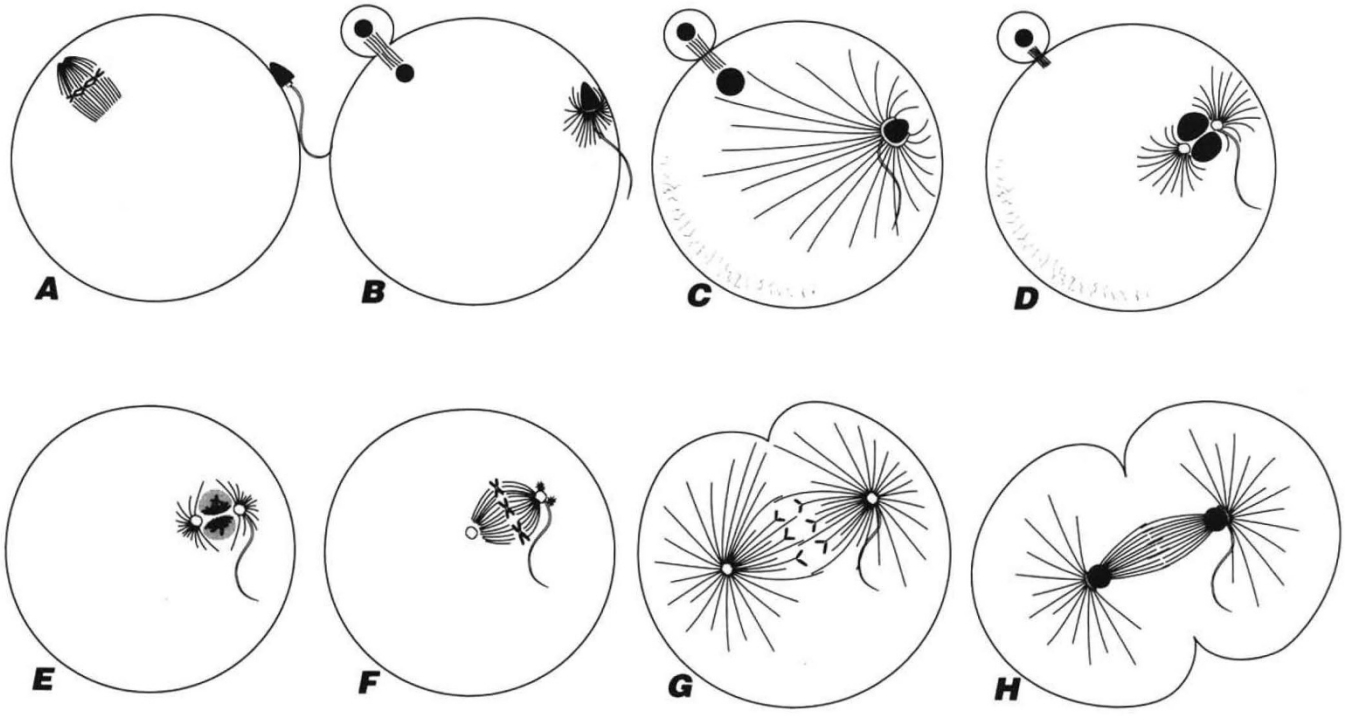

Fig. 3 Microtubule organization and centrosome behaviour during fertilization in humans, and the stages at which human fertilization arrests. Unfertilized oocytes have microtubules only within the metaphase-arrested second meiotic spindle *a*. After introduction of the sperm centrosome following sperm incorporation *b*, new microtubules assemble to form the radial sperm aster adjacent to the decondensing male pronucleus *b*. Centrosome position and shape is inferred from the observed pattern of microtubules. Microtubules are also found in the meiotic midbody *b–d*, and as disarrayed fibres in the cytoplasm distal to the sperm aster *c–d*. As male and female pronuclei decondense *c*, the sperm aster enlarges, and the male pronucleus is displaced centripetally. The female pronucleus moves toward the male *d* as the sperm aster becomes asymmetric and bipolar. Two microtubule tufts emanate from apposed pronuclei *d*, suggesting that centrosome splitting occurs late in interphase. The still-separate maternal and paternal chromosomes condense at prophase *e*. They align during prometaphase, so that by metaphase *f*, parental genomes have united at the spindle equator. One or two small asters form at the metaphase spindle pole with the sperm tail *f*. Pronuclei remain eccentric until first anaphase *g*, when asters enlarge and preferentially interact with the adjacent cortical region; this displaces the spindle toward the zygote center. The cleavage furrow initially forms at this site, suggesting that sperm aster placement plays a role in specification of the first cleavage axis *h*. The events past metaphase are inferred from studying rhesus zygotes (Wu, G.-J. *et al.*). Defects observed in oocytes from infertile patients include failures to complete: (1) sperm incorporation, egg activation, and/or exiting of second meiosis (*a–b*); (2) sperm aster nucleation *b*; (3) aster enlargement and pronuclear decondensation *c*; (4) coordinated centration of male pronucleus with sperm astral microtubules and sperm tail (*b–c*); (5) migration of female pronucleus (*c–d*); and (6) cell-cycle progression (meiosis to interphase (*a–b*); interphase to mitosis (*e–f*); or mitotic metaphase to interphase (*f–h*)).